Engineered Polymeric Nanoparticles for Receptor-Targeted Blockage of Oxidized Low Density Lipoprotein Uptake and Atherogenesis in Macrophages

Evangelia Chnari,[†] Jessica S. Nikitczuk,[‡] Jinzhong Wang,[§] Kathryn E. Uhrich,[§] and Prabhas V. Moghe*[,†,‡]

Department of Biomedical Engineering, Department of Chemical and Biochemical Engineering, and Department of Chemistry and Chemical Biology, Rutgers University, Piscataway, New Jersey 08854

Received January 29, 2006; Revised Manuscript Received April 3, 2006

Strategies to prevent the uptake of modified low density lipoproteins (LDLs) by immune cells, a major trigger of inflammation and atherogenesis, are challenged by complex interfacial factors governing LDL receptor-mediated uptake. We examine a new approach based on a family of "nanoblockers", which are designed to examine the role of size, charge presentation, and architecture on inhibition of highly oxidized LDL (hoxLDL) uptake in macrophages. The nanoblockers are macromolecules containing mucic acid, lauryl chloride, and poly(ethylene glycol) that self-assemble into 15−20 nm nanoparticles. We report that the micellar configuration of the macromolecules and the combined display of anionic (carboxylate) groups in the hydrophobic region of the nanoblockers caused the most effective inhibition in the uptake of hoxLDL by IC21 macrophages. The nanoblockers primarily targeted SR-A and CD36, the major scavenger receptors and modulated the "atherogenic" phenotype of cells in terms of the degree of cytokine secretion, accumulation of cholesterol, and "foam cell" formation. These studies highlight the promise of synthetically engineered nanoblockers against oxidized LDL uptake.

Introduction

Atherosclerosis represents an inflammatory response of macrophages to invading pathogenic lipoproteins in the arterial wall.[1] The earliest visible atherosclerotic lesions, fatty streaks, consist mainly of macrophages that have taken up excessive amounts of cholesterol. During the early stages of atherosclerosis, lipoproteins from the circulating blood infiltrate into the intima and accumulate in the arterial wall. In response to the lipid accumulation, monocytes migrate into the intima, where they differentiate into macrophages.[2] Differentiation of monocytes to macrophages leads to upregulation of scavenger receptors on the cell surface. Scavenger receptors recognize the altered molecular patterns of oxidized LDL and lead to an uncontrolled uptake and intracellular accumulation of cholesterol, characteristic of foam cells.

A wide range of scavenger receptors, class A, B, C, D, and E receptors, mediates the uptake of oxidized LDL by macrophages, the specificity varying with the degree of oxidative modification of LDL.[3,4] Class A scavenger receptors SRAI/II are found in the arterial wall, primarily expressed in lesion macrophages,[5] and have been shown to bind oxidized LDL[6,7] through the C-terminal 22 amino acids of the collagen-like domain.[2] Class B scavenger receptors, SR-BI and CD36[8−10] as well as class D macrosialin/CD68 can also mediate the uptake and degradation of oxidized LDL.[11] Among these receptors, SRA and CD36 appear to be of primary importance in atherogenesis and mice lacking either receptor show considerable reduction in lesion formation.[10,12] Lipoprotein internalization via scavenger receptors is not regulated by intracellular cholesterol content[13,14] and can lead to excessive accumulation of cholesteryl esters in the cytoplasm,[2] thus contributing to the formation of foam cells.[14,15]

There is strong evidence that oxidized forms of LDL, especially highly oxidized LDL, are present in arterial lesions[5] and play a role in foam cell formation.[16] Oxidation of LDL is also associated with the formation of a number of highly reactive molecules, such as lipid peroxides, lysoPC, oxysterols, and aldehydes, which interact with surrounding cells and cause nonspecific activation or even death.[17] Cholesterol-loaded macrophages also play a role in the activation of smooth muscle cells (SMCs), by secreting cytokines and growth factors that enhance SMC proliferation, leading to development of fibromuscular plaques or restenosis after surgical intervention.[17] Although clearance of the highly atherogenic oxidized LDL is important for protection of the surrounding tissue from damage, the unregulated uptake of hoxLDL by macrophages in the arterial wall leads to conversion of macrophages into lipid-filled foam cells, which marks the initiation of atherosclerotic lesions.

Research has been done previously on the discovery of synthetic compounds that can act as high affinity scavenger receptor inhibitors, blocking modified LDL entry in cells.[18,19] Sulfatide derivatives have been synthesized to be used as blockers of scavenger receptor A and have been shown to reduce acetylated LDL binding and uptake in a concentration-dependent manner.[19] In addition, synthetic oxidized phospholipids (oxidized phosphocholine) cross-linked to bovine serum albumin or a hexapeptide have been used as pattern recognition ligands for CD36. These synthetic ligands have been shown to competitively inhibit the binding of oxidized LDL to CD36-transfected cells.[18] Although previous attempts to develop scavenger receptor inhibitors have been encouraging, using a 3-D presentation of the targeting moieties to increase efficiency of the inhibitors has not been investigated. In addition, the compounds

* To whom correspondence should be addressed. Phone: 732-445-4951. Fax: 732-445-2581. E-mail: Moghe@rci.rutgers.edu.
[†] Department of Chemical and Biochemical Engineering.
[‡] Department of Biomedical Engineering.
[§] Department of Chemistry and Chemical Biology.

10.1021/bm0600872 CCC: $33.50
Published on Web 05/10/2006

synthesized are not multifunctional but are targeting a specific scavenger receptor, whereas the rest of the scavenger receptors on the cell may continue to mediate internalization of modified LDL.

Our studies focus on anionic amphiphilic macromolecules that spontaneously form micelles (referred to as nanoparticles in this paper) at concentrations above the critical micelle concentration.[20] These nanoparticles present the anionic charges in an organized, clustered form for better efficiency and have the potential of drug encapsulation[21,22] for various therapeutic applications. In our previous study, we demonstrated that anionic amphiphilic nanoparticles inhibit oxidized LDL uptake by macrophages in a concentration dependent manner.[23] In this study, we investigated the mechanistic basis for this inhibition in IC21 macrophages. We report that the anionic nanoparticles can inhibit the IC21 cell uptake of the most atherogenic form of LDL by blocking two primary scavenger receptors. Further, we demonstrate that the nanoparticle-mediated inhibition of highly oxidized LDL uptake can effectively retard accumulation of cholesterol and the development of a foam cell phenotype, as well as lower the secretion of the inflammatory cytokine TNF-α.

Materials and Methods

Lipoprotein Model: LDL Oxidation. LDL purified from human plasma (Molecular Probes, Eugene, OR) was employed for all of the experiments in this study. Oxidized LDL was prepared and characterized via methods elaborated in our earlier study.[24] Highly oxidized LDL was generated by incubating 50 μg/mL LDL with 10 μM $CuSO_4$ at 37 °C for 18 h exposed to air.[25,26] The oxidation was terminated with an aqueous solution of 0.01% w/v ethylenediaminetetraacetic acid (EDTA) (Sigma, St. Louis, MO). The extent of LDL oxidation was characterized as the content of conjugated dienes,[27,28] lipid peroxides,[29] and thiobarbituric acid reactive substances (TBARS)[27,30] as well as by monitoring LDL electrophoretic mobility (REM), which correlates with the overall change in the LDL particle charge.[31,32] In our experiments, the REM value of highly oxidized LDL was 3.6 compared to the value of REM of 1.0 for native LDL.[24]

Synthesis and Characterization of the Nanoparticles. Heterobifunctional poly(ethylene glycol) (NH_2−PEG-COOH) with molecular weights of 5000 Da was obtained from Nektar (San Carlos, CA). 4-(Dimethylamino)pyridinium *p*-toluenesulfonate (DPTS) was prepared as previously described.[20] Carboxylate-terminated poly(ethylene glycol) (PEG-COOH)) with a molecular weight of 5000 Da was purchased from Sigma-Aldrich. All PEG reagents were dried by azeotropic distillation with toluene. All other reagents and solvents were purchased from Aldrich and used as received.

Details about the synthesis and characterization of amphiphilic scorpion-like macromolecules (AScMs) as anionic nanoparticles with carboxylates on hydrophobic domains (MCOOH, polymer **1**) used for our experiments were previously published.[20,33] In brief, the hydroxyl groups of mucic acid were acylated using dodecanoyl chloride in the presence of catalytic zinc chloride, and then monohydroxyl-substituted PEG of molecular weight 5000 Da was coupled using 1,3-dicyclohexylcarbodiimide (DCC) and DPTS as catalyst to yield the anionic nanoparticles with the carboxylate in the hydrophobic domain (MCOOH). Similarly, the ethoxy-terminated AScMs (NM, polymer **2**) as control nanoparticles were prepared by esterification of polymer **1** (MCOOH) with ethyl alcohol using DCC and catalyst DPTS (Figure 1(II)).

Synthesis of the carboxylic acid-terminated AScMs on the hydrophilic domain (polymer **5**, PCOOH) has not been published before and is described here in more detail. For the synthesis of PCOOH (Figure 1(II)), M (12) derivative **3** (0.937 g, 1.0 mmol) was activated to **4** by *N*-hydroxysuccinimate (NHS) (0.276 g, 2.4 mmol) in dichloromethane (20 mL) and dimethyl sulfoxide (2 mL) with 1 M DCC dichloromethane solution (2.4 mL, 2.4 mmol) as dehydrating reagent. Intermediate **4** was obtained as a white solid, (1.0 g, 88.8% yield). Then, NH_2−PEG-COOH (1.0 g, 0.2 mmol) was coupled with **4 (**0.452 g, 0.4 mmol) in dichloromethane (10 mL) and triethylamine (1.0 mL, 9.3 mmol) to obtain polymer **5**. The product was obtained as a white, waxy solid (0.92 g, 90.2% yield). The molecular structure of the synthesized amphiphilic macromolecules (PCOOH) was confirmed by ^{1}H and ^{13}C NMR spectroscopies on Varian 400 MHz spectrometers using samples (∼5−10 mg/mL) dissolved in $CDCl_3$-*d* solvent and tetramethylsilane as the reference signal. The ethylene oxide of PEG comprises a significant component and dominates the NMR spectra. ^{1}H NMR ($CDCl_3$) (δ): 8.17 (s, 1H, N*H*-C═O), 5.95 (m, 2H, C*H*), 5.55 (m, 2H, C*H*), 3.63 (m, ∼0.4kH, CH_2), 2.79 (t, 4H, CH_2), 2.49 (t, 4H, CH_2), 2.37 (t, 4H, CH_2), 1.63 (m, 4H, CH_2), 1.58 (m, 4H, CH_2), 1.25 (m, 64H, CH_2), 0.87 (t, 12H, CH_3). ^{13}C NMR ($CDCl_3$): δ 171.95 (*C*═O), 170.34 (*C*═O), 163.16 (*C*═O), 72.01 (*C*H_2−O), 70.73 (*C*H_2−O, dominant), 69.045 (*C*H_2−O), 68.840 (*C*H_2−O), 33.85 (*t-C*H), 29.66 (*C*H_2), 29.52 (*C*H_2), 25.64 (*C*H_2), 22.85 (*C*H_3).

Gel permeation chromatography (GPC) was used to obtain the molecular weight and the polydispersity index (PDI). For polymer **5**, M_w = 6.3k Da and PDI = 1.07. Gel permeation chromatography was performed on a Perkin-Elmer Series 200 LC system equipped with Pl gel column (5 μm, mixed bed, ID 7.8 mm, length 300 mm) and with a Water 410 refractive index detector, Series 200 LC pump, and ISS 200 Autosampler. A Digital Celebris 466 computer was used to automate the analysis via PE Nelson 900 interface and PE Nelson 600 Link box. Perkin-Elmer Turbochrom 4 software was used for data collection as well as data processing. Tetrahydrofuran (THF) was the eluent for analysis and solvent for sample preparation. The sample was dissolved in THF (∼5 mg/mL) and filtered through a 0.45 μm PTFE syringe filter (Whatman, Clifton, NJ) before injection into the column at a flow rate of 1.0 mL/min. The average molecular weight of the sample was calibrated against narrow molecular weight polystyrene standards (Polysciences, Warrington, PA).

Critical micelle concentration (CMC) studies in aqueous solutions were carried out on a Spex fluoroMax Spectrofluorometer (Piscataway, NJ) at 25 °C by using pyrene as the probe molecule. Pyrene maximum absorption shifted from 332 to 334.5 nm upon secondary micelle formation. The ratio of absorption of polymer (334.5 nm) to pyrene only (332 nm) was plotted as the logarithm of polymer concentrations. The inflection point (CMC) of the curves was 1.03×10^{-6} M.

Dynamic light scattering (DLS) was utilized to determine the micelle size and distribution; the nanoparticles were unimodal and very stable upon dilution. All subsequent experiments were performed at concentrations above the CMC. Dynamic light scattering (DLS) analyses were performed by photon correlation spectroscopy using a PSS Nicomp 380 submicron particle sizer instrument (Particle Sizing Systems, Santa Barbara, CA). A 20 mW, 523 nm diode-pumped solid-state laser module and an avalanche photodiode detector were used. Polymer solutions (1 wt %) in three different buffered aqueous solutions were prepared. Solutions were prepared at pH 2.0 (0.01 N HCl), 7.4 (PBS), and 9.0 (sodium carbonate). Measurements were performed at a 90° scattering angle at 25 °C. Nicomp number-weight analysis and multimodal Laplace transform analysis were used to process data.

Cell Culture. Nanoparticle and LDL uptake studies were conducted using mouse IC21 peritoneal macrophage cell line (IC21) (ATCC, Manassas, VA), which was propagated in culture using RPMI-1640 media (ATCC, Manassas, VA) containing 10% fetal bovine serum (FBS) (Gibco-Invitrogen, Carlsbad, CA) and 1% penicillin/streptomycin (Biowhittaker, Walkersville, MD). The cells were harvested at confluence, and 10 000 cells/well were re-cultured in 96-well tissue culture plates for 5 days, prior to experimental use. IC21 sub-lines were propagated for a maximum of 8 weeks.

Regulation of hoxLDL Uptake by IC21 Macrophages. The uptake behavior of fluorescently labeled LDL-BODIPY (Molecular Probes, Eugene, OR) by IC21 macrophages was investigated in the presence or absence of nanoparticles. Three anionic macromolecules were

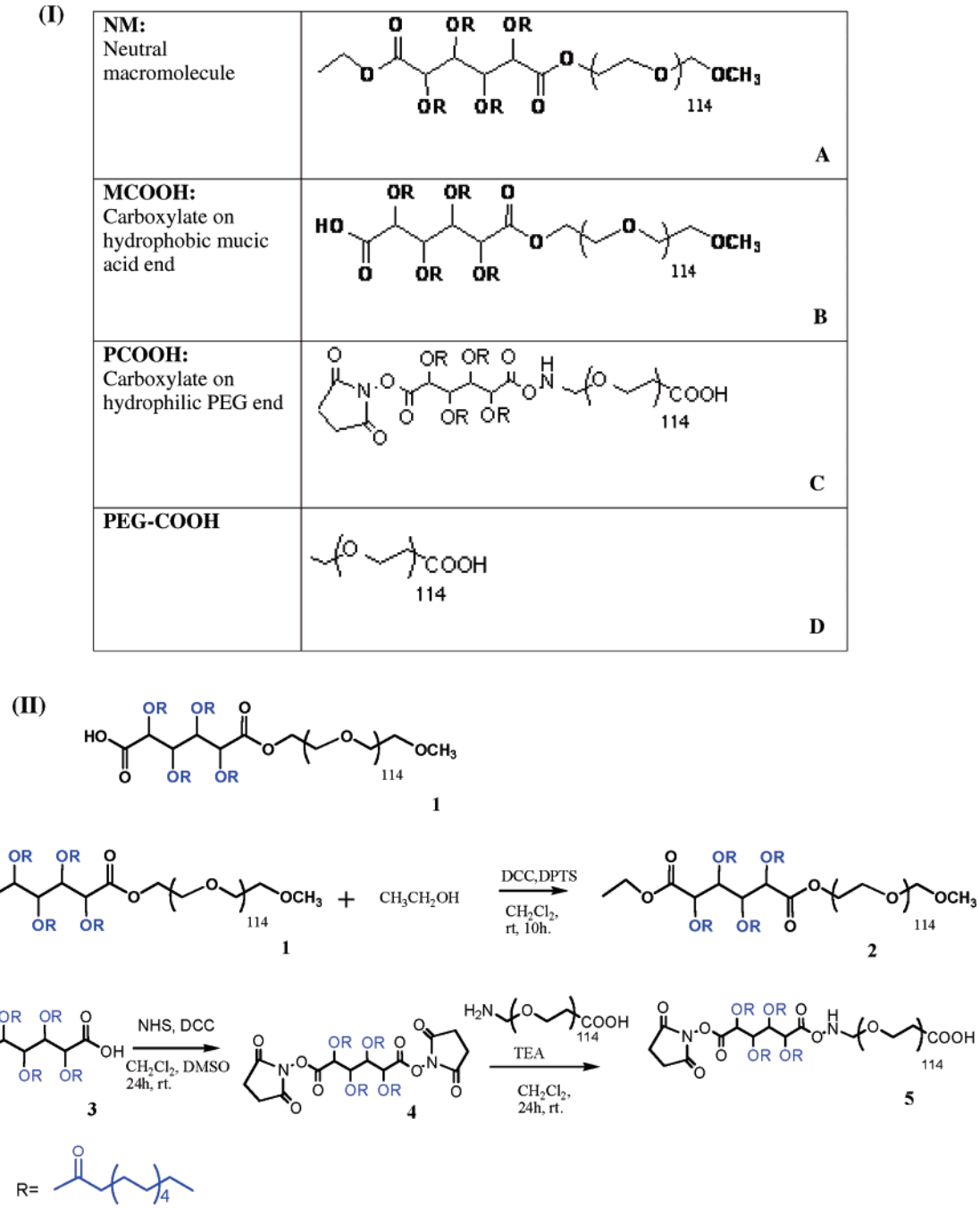

Figure 1. Structure and synthetic scheme of the nanoparticles. (I) Structure of uncharged ethoxy-terminated nanoparticles (neutral macromolecules, NM) (**A**); anionic nanoparticles with the carboxylate on the hydrophobic chain end, MCOOH (**B**); anionic nanoparticles with the carboxylate at the hydrophilic end, PCOOH (**C**); and control macromolecules that do not form nanoscale micelles, PEG-COOH (**D**). (II) Synthetic scheme of uncharged and PCOOH nanoparticles.

evaluated: (i) MCOOH that contain a carboxylic acid in the hydrophobic domain, (ii) PCOOH that contain a carboxylic acid in the hydrophilic PEG domain, and (iii) carboxylate-terminated PEG that cannot form micelles (Figure 1(I)). A neutral micelle-forming macromolecule (NM) of similar chemical structure as MCOOH and PCOOH was utilized as the control.

For the uptake experiments, 10 μg/mL labeled highly oxidized LDL-BODIPY, preincubated with macromolecules, was incubated with IC21 cells for 5 h at 37 °C in a humidified incubator with 5% CO_2. The cells were washed twice with serum-free RPMI containing 0.4% bovine serum albumin (BSA) (Sigma, St. Louis, MO) and then twice with serum-free RPMI. The cell-associated fluorescence was measured by capturing images on a Zeiss epifluorescence microscope (Sun Microsystems, Santa Clara, CA), the fluorescence intensity was quantified using Image Pro Plus 5.1 software (Media Cybernetics, San Diego, CA), and LDL uptake was normalized to the uptake in the absence of blocking or nanoparticles. High magnification images (80×) were also captured for a visual confirmation of the effect of nanoparticles on hoxLDL uptake.

Fluorescent Labeling of Nanoparticles. The anionic nanoparticles were fluorescently labeled with cationic Texas Red hydrazide dye (Molecular Probes, Eugene, OR), using carbodiimide chemistry. Briefly, to a polymer solution (10^{-4} M) was added a 10 M excess of 1-ethyl-3-(3-dimethylaminopropyl)carbodiimide hydrochloride (EDC) (Advanced ChemTech, Louisville, KY) and a 10 M excess Texas Red in *N*,*N*-dimethylformamide (DMF) (Sigma, St. Louis, MO). The reactants were incubated overnight while stirring. The solution was dialyzed at 4 °C for 24 h through 3500 MWCO regenerated cellulose dialysis tubing (wet in 0.1% sodium azide) (Spectrum Labs, Rancho Dominguez, CA). For cellular uptake studies, a 5% solution of the fluorescently labeled

nanoparticles was mixed with nonfluorescent anionic nanoparticles, dissolved in serum-free RPMI. Uncharged labeled nanoparticles at similar concentrations were mixed with nonfluorescent nanoparticles and used as controls.

Scavenger Receptor Expression on IC21 Macrophages. The expression of scavenger receptors on IC21 murine macrophages was verified via indirect immunofluorescence and flow cytometry. The antibodies used for our studies were (a) 2F8 monoclonal rat anti-mouse class A receptor antibody (Accurate Corp., NY) and (b) monoclonal antibody to clone 63 of CD36 receptors (Cascade BioScience, MA). Cells were preincubated with 10 μg/mL antibodies for 30−45 min at 4 °C, washed 3 times with serum-free RPMI, and then incubated with fluorescently labeled secondary antibodies (FITC-conjugated goat anti-rat and donkey anti-mouse (Jackson ImmunoResearch, PA)) for 1 h at 4 °C to allow for binding. Cells were then washed twice and fixed in a 0.5% formaldehyde (Sigma, St. Louis, MO) solution for 20 min at room temperature, and the receptor expression was monitored using flow cytometry (FACS, BD Biosciences, San Jose, CA) and fluorescence microscopy.

Scavenger Receptors Involved in the Cell−Nanoparticle Interactions. The role of class A and class B scavenger receptors in the interactions between nanoparticles and cells were studied using two complementary approaches: (i) macrophage preincubation with nanoparticles and subsequent addition of receptor-specific antibodies to monitor the competitive ability of nanoparticles to block antibody-receptor binding and (ii) receptor blocking with antibodies to isolate how selected receptors influence uptake of nanoparticles by macrophages. In both cases, Texas-Red-labeled nanoparticles were used. In the first case, macrophages were incubated with 10^{-5} M labeled nanoparticles for 2 h at 4 °C, washed twice with serum-free RPMI, and then incubated with 10 μg/mL primary antibodies to SR-A and CD36 (mentioned before) for 45 min at 4 °C. The cells were washed twice with serum-free RPMI and incubated with the respective secondary antibodies for 1 h at 4 °C. The cells were washed again and imaged at 63× magnification under the Leica TCS SP2 microscope (Leica Microsystems, Exton, PA) for qualitative evaluation of the nanoparticle interference in the antibodies binding to the cell receptors.

The role of scavenger receptors in nanoparticle uptake by macrophages was quantitatively determined by incubating the cells with 10 μg/mL primary antibodies to SR-A and CD36 for 45 min at 37 °C to block receptor availability. The cells were then incubated with fluorescently labeled nanoparticles for 2 h at 37 °C in the presence of antibodies to ensure continuous receptor blocking. Cells were washed with serum-free RPMI before imaging on a Zeiss epifluorescence microscope (Sun Microsystems, Santa Clara, CA). The relative involvement of SR-A and CD36 scavenger receptors in IC21 cell uptake of nanoparticles was determined using Image-Pro Plus 5.1 software (Media Cybernetics, San Diego, CA) for quantification of the cell-associated nanoparticle fluorescence intensity.

Receptor-Mediated LDL Uptake Mechanisms. Receptor-mediated mechanisms of fluorescently labeled hoxLDL uptake by macrophages were investigated using antibody-blocking experiments. After receptor blocking by antibodies described above, cells were incubated with 10 μg/mL fluorescently labeled hoxLDL-BODIPY (Molecular Probes, Eugene, OR) in the presence or absence of nanoparticles for 2 h at 37 °C. Antibodies were also included during the cell incubation with hoxLDL to ensure that the receptors remain blocked during the entire incubation period. Cells were washed with serum-free RPMI before imaging. For each experimental condition, the levels of uptake elicited by hoxLDL in the absence of nanoparticles and receptor blocking were used as the baseline. The relative contributions of class A and class B scavenger receptors for IC21 cell uptake of highly oxidized LDL were determined using Image-Pro Plus 5.1 software (Media Cybernetics, San Diego, CA) for quantification of the cell-associated LDL fluorescence intensity.

Foam Cell Formation. Foam cell formation was qualitatively estimated via light microscopy. The cellular morphology after treatment with highly oxidized LDL in the presence or absence of nanoparticles was observed. Cells were incubated with 40 μg/mL highly oxidized LDL for 24 h at 37 °C in the absence of nanoparticles or in the presence of 10^{-6} M uncharged or anionic nanoparticles. Transmitted images of the cells were captured with a Zeiss confocal microscope (Sun Microsystems, Santa Clara, CA).

Cholesterol Content. Cholesterol accumulation within cells exposed to hoxLDL was assessed in the presence or absence of nanoparticles using the Amplex Red Cholesterol assay kit (Molecular Probes, Eugene, OR). Cells were incubated with 40 μg/mL hoxLDL for 12 h at 37 °C in the presence or absence of nanoparticles. After the incubation, the cells were washed twice with serum-free RPMI. The cholesterol was extracted by incubating the cells with a 3:2 mixture of hexane:2-propanol for 30 min at room temperature. The wells were dried under nitrogen, and the procedure was repeated. The extracted cholesterol was resuspended in reaction buffer (from the kit) by incubating the well plate at 37 °C for 15 min and periodically shaking on a plate rocker. The cholesterol quantification method used is based on an enzyme-coupled reaction that detects both free cholesterol and cholesteryl esters. Cholesteryl esters are hydrolyzed by cholesterol esterase into cholesterol, which is then oxidized by cholesterol oxidase to yield hydrogen peroxide and a ketone product. The hydrogen peroxide was detected fluorometrically using 10-acetyl-3,7-dihydroxyphenoxazine (Amplex Red reagent), a highly sensitive and stable probe for hydrogen peroxide.

Tumor Necrosis Factor Alpha (TNF-α) Secretion. Cytokine secretion by macrophages after incubation with highly oxidized LDL was quantified in the presence or absence of nanoparticles. Cells were incubated with 5 μg/mL highly oxidized LDL for 6 h (previously shown to be an appropriate time and concentration for macrophage activation by hoxLDL[34,17]) in the absence or presence of anionic and uncharged nanoparticles. The supernatants were collected and the amount of secreted TNF-α was quantified using a commercially available ELISA kit (Pierce, Rockford IL).

Results

LDL Uptake Studies in IC21 Macrophages: Role of the Positioning of the Anionic Group on the Nanoparticles. We investigated the effect of anionic or control (uncharged) nanoparticles on the macrophage internalization patterns of highly oxidized LDL. We first compared nanoparticles wherein the anionic group was embedded within the hydrophobic part (MCOOH) to nanoparticles wherein the anionic group was embedded within the hydrophilic part (PCOOH), Figure 1(I). Control conditions comprised uncharged nanoparticles (NM) and carboxylate groups attached to PEG chains (PEG-COOH) of the same chain length as for the nanoparticles. The hydrophobic-bound carboxylate group was the most efficient, causing a 75% inhibition in hoxLDL uptake compared to only 34% induced by the hydrophilic-bound carboxylate (Figure 2(I)). The PEG-COOH macromolecules, which do not self-assemble into nanoparticles, did not have any effect in inhibiting hoxLDL uptake by macrophages, which signifies the role of the organization and clustering of the anionic charges in the efficiency of the inhibition. As the MCOOH nanoparticles were proven the most effective, they were used for the remaining experiments. Images of the intracellular levels of highly oxidized LDL in the absence of nanoparticles and in the presence of uncharged as well as anionic nanoparticles are shown in Figure 2(II). Uncharged nanoparticles had a basal effect in inhibiting hoxLDL uptake, which was dramatically enhanced in the presence of anionic nanoparticles (MCOOH).

Receptor Expression and Blocking Experiments. First, we verified the expression of scavenger receptors SR-A and CD36 on the surface of IC21 macrophages using immunolocalization.

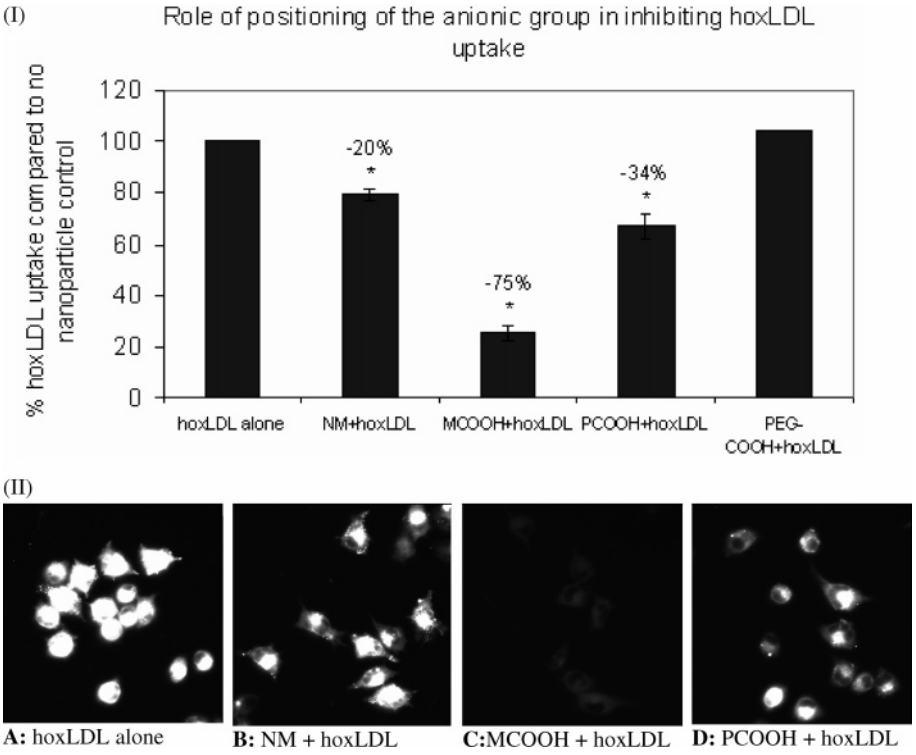

Figure 2. Role of the carboxylate group position in the inhibition of hoxLDL uptake. (I) MCOOH and PCOOH nanoparticles at concentrations of 10^{-6} M were preincubated with fluorescently labeled hoxLDL-BODIPY for 12 h before addition to IC21 macrophages for 5 h at 37 °C. PEG-COOH, uncharged nanoparticles (NM) and no nanoparticle (blank) conditions were used as controls. Lipoprotein uptake in each case was quantified using fluorescence microscopy and densitometry. The experiment was repeated 2−3 times in triplicate. Statistical analysis was done using ANOVA single factor ($P < 0.05$). The percentages represent the reduction in hoxLDL uptake compared to hoxLDL alone. (II) Fluorescent (bottom panel) images of internalized hoxLDL-BODIPY in IC21 macrophages in the absence (A) or presence of uncharged (B), MCOOH (C), or PCOOH (D) nanoparticles. The dramatic effect of MCOOH is also confirmed visually.

With the use of both microscopy and flow cytometry (Figure 3), the expression of scavenger receptor A and CD36 on the surface of IC21 macrophages was confirmed. The interaction between the nanoparticles (red fluorescence) and macrophage scavenger receptors were qualitatively determined by examining the effect of nanoparticle preincubation of macrophages on subsequent antibody (green fluorescence) binding to specific receptors (Figure 4(I)). Preincubation with uncharged nanoparticles did not significantly reduce subsequent antibody-receptor binding, whereas the carboxylate-functionalized nanoparticles significantly reduced antibody binding (less green and more red fluorescence was observed compared to uncharged controls) and/or co-localized with the antibodies producing a yellow fluorescence. To clarify the internalization pathways of differentially oxidized LDL and the function of nanoparticles in controlling the uptake process, selected receptor blocking experiments were performed. First, the role of certain scavenger receptors in the uptake of Texas Red fluorescently labeled anionic and uncharged nanoparticles was assessed (Figure 4(II)). Scavenger receptor A blocking led to reduced internalization of the anionic nanoparticles, which signifies a potential mechanism for nanoparticle uptake. The blocking reduced uptake by only 30%, implying the role of other pathways in the uptake of the anionic nanoparticles. None of the receptors tested were apparently involved in the uptake of the uncharged nanoparticles. Various scavenger receptors seem to influence, at different degrees, highly oxidized LDL uptake by macrophages (Figure 5). Scavenger receptor A and CD36 were the most important contributors, the blocking of which reduced hoxLDL uptake by 26% and 35%, respectively. Simultaneous blocking of both receptors led to an 83% reduction in highly oxidized LDL uptake, indicating that these two receptors cooperatively are the main players in highly oxidized LDL uptake by IC21 macrophages. The anionic nanoparticle inhibition of uptake via scavenger receptors was confirmed by our experiments wherein both anionic nanoparticles and highly oxidized LDL are present. Anionic nanoparticles appeared to inhibit hoxLDL uptake mediated via SR-A and CD36 scavenger receptors, as simultaneous blocking of both receptors caused equal reduction in hoxLDL uptake as in the case of anionic nanoparticles alone. Blocking of each receptor separately with the respective antibody, in the presence of the anionic nanoparticles, did not cause any significant additional reduction in hoxLDL uptake compared to the no blocking control condition. Simultaneous blocking of the two receptors led to a further inhibition in hoxLDL uptake indicating cooperative involvement of these scavenger receptors during the interactions of the anionic nanoparticles with the cells. The uncharged nanoparticles (NM) also seemed to cause a basal inhibition to hoxLDL uptake. Since the scavenger receptors tested are not involved in NM−macrophage interactions, the inhibitory effect potentially occurs via blocking of other receptors and/or of more nonspecific internalization routes, including via lipid rafts and pinocytosis.

Cholesterol Content: Foam Cell Formation. Intracellular cholesterol accumulation is important in foam cell formation. We examined the effect of the anionic nanoparticles in modulating cholesterol deposition. In a manner similar to hoxLDL internalization, total cholesterol accumulation in macrophages due to incubation with atherogenic lipoproteins was reduced in the presence of anionic nanoparticles by more than 3-fold (Figure 6(I)). This effect is also observed in the cell morphology, where the cells that were incubated only with hoxLDL had a foamy appearance, whereas in the presence of the nanoparticles

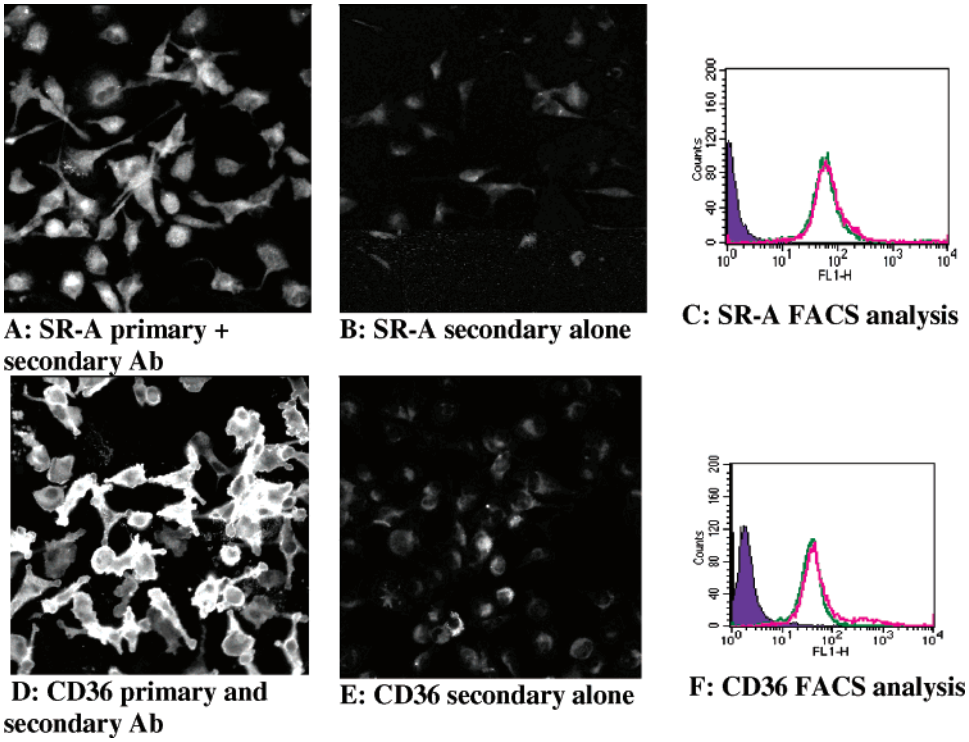

Figure 3. Scavenger receptor expression on IC21 macrophages. Cells were incubated with 10 μg/mL primary antibodies to SR-A (A) and CD36 (D) for 30−45 min at 4 °C to block the specific receptors. Then, the secondary antibodies (10 μg/mL) were added for 1 h at 4 °C. Controls with secondary antibodies alone (B and E, respectively) were used to account for the nonspecific binding. Receptor expression was analyzed using fluorescence microscopy (A and B and D and E) and confirmed by flow cytometry (C and F). In the flow cytometry graphs the purple histograms represent cells with secondary antibodies (nonspecific binding), the green histograms receptor expression at 4 °C and the red ones at 37 °C.

(especially anionic ones), the foam cell phenotype was significantly reduced (Figure 6(II)).

TNF-α Secretion. The inhibitory effect of the anionic nanoparticles on the secretion of oxLDL-induced TNF-α was also shown performing ELISA on the supernatants of cells conditioned with hoxLDL in the presence or absence of the nanoparticles. Anionic nanoparticles reduced TNF-α secretion by more than 50% compared to hoxLDL alone, approaching the low levels of controls where hoxLDL was absent (Figure 7). The nanoparticle controls in the absence of hoxLDL did not activate TNF- α secretion. Fucoidan was used as a positive control, as it has previously been shown to considerably increase secretion of TNF-α by macrophages.[34]

Discussion

Uncontrolled uptake of oxidized forms of LDL by vascular cells leads to intracellular accumulation of cholesterol and foam cell formation, one of the first steps in the escalation of atherogenesis. In our previous study, we showed that synthetically designed amphiphilic scorpion-like macromolecules, presenting glycosoaminoglycan-mimetic anionic groups, can differentially reduce the internalization of oxidized LDL within IC21 macrophages.[23] In the current study, we report that the carboxylic acid-terminated nanoparticles can effectively inhibit highly oxidized LDL uptake primarily through scavenger receptor blocking and reduce cholesterol accumulation and foam cell conversion within IC21 macrophages. Two key structural features of the macromolecules appear to be essential for scavenger receptor-based inhibition of hoxLDL uptake: the proximity of the anionic groups to the hydrophobic core of the nanoparticles and the 3-D organization/clustering of the amphiphilic groups and charges in a micellar form.

To optimize the nanoparticles for maximal inhibition of hoxLDL uptake, we compared the efficacy of nanoparticles with the carboxylate attached to the hydrophobic region (MCOOH) to nanoparticles with the carboxylate attached to the hydrophilic region (PCOOH). Our results demonstrate the significantly better ability of MCOOH to inhibit highly oxidized LDL uptake by 75%, compared to 34% for PCOOH. This behavior may be due to the hydrophobic interactions acting in cooperation with the charge interactions, thus enhancing the anionic nanoparticle binding to the receptor and improving its inhibitory ability. The role of anionic groups and lipophilic moieties in blocking scavenger receptor A has been previously demonstrated by Yoshiizumi et al.,[19] who studied a range of sulfatide derivatives consisting of two lipophilic chains, a peptide structure replacing ceramide, a phenylene moiety replacing galactose and sulfate or carboxylic anionic groups. They investigated each molecule's ability to inhibit binding of acetylated LDL to macrophages via scavenger receptor A and verified that inhibitory activity required both anionic groups and the presence of hydrophobic chains. Boullier et al.[18] used peptide adducts to an oxidation product of phosphocholine (PC) on oxidized LDL, recognized by CD36 receptors,[35] as inhibitors of oxidized LDL binding to CD36 on COS-7 cells.[18] The lipid environment and the structural elements of the oxidized PC molecule were necessary to maintain the appropriate conformation and presentation of PC to be recognized as a ligand.[18] However, organized presentation of multiple anionic charges in the form of amphiphilic nanoparticles for scavenger receptor inhibition has not, to our knowledge, been systematically investigated. The importance of the 3-D organization and clustering of the anionic charges was demonstrated with the inclusion of PEG-COOH; this control macromolecule has the same anionic charge density as the other nanoparticles (MCOOH and PCOOH) but does not self-

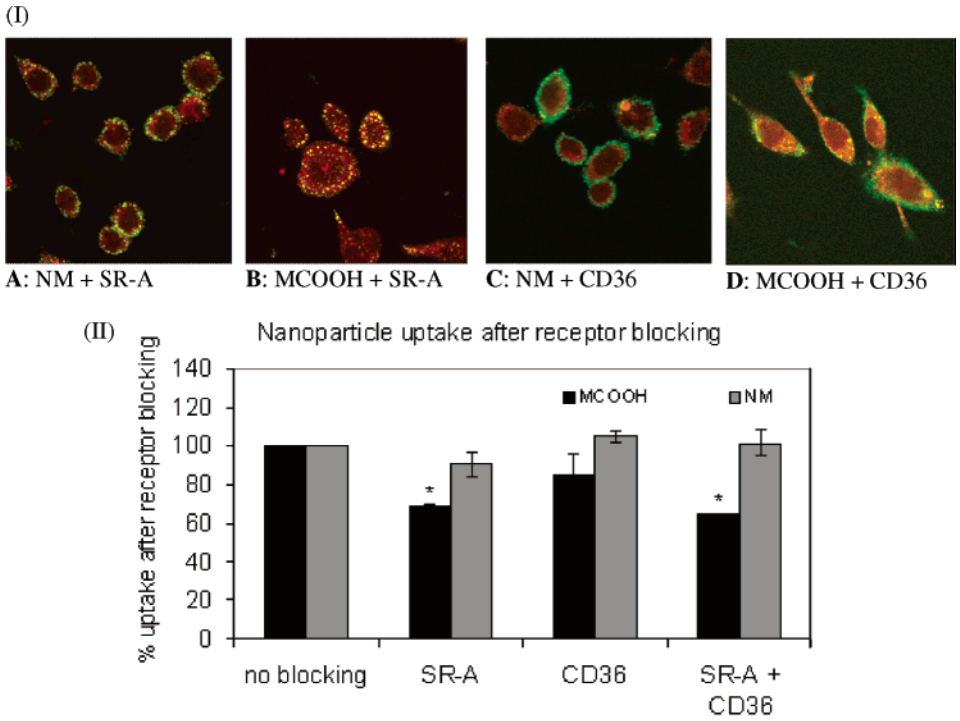

Figure 4. Scavenger receptors involved in nanoparticle interactions with IC21 macrophages. (I) Visualization of the nanoparticle interactions with scavenger receptors. Cells were preincubated with Texas-Red-labeled NM and MCOOH for 2 h at 4 °C and then antibodies to SR-A or CD36 were added to the cells for 30−45 min at 4 °C. Fluorescently labeled (FITC) secondary antibodies were added for 1 h at 4 °C for visualization of the blocked receptors. (II) Receptor-mediated pathways involved in the nanoparticle uptake by IC21 macrophages. Cells were incubated with 10 μg/mL primary antibodies to SR-A and CD36 as well as a combination of the two for 30−45 min at 37 °C to block the respective receptors. Then, fluorescently labeled nanocarriers were added to the cells for 2 h at 37 °C, in the presence of 10 μg/mL primary antibodies to avoid depletion during the incubation period. Controls of no receptor blocking were used. Nanoparticle uptake in each case was quantified using fluorescence microscopy and densitometry. The experiment was repeated 2 times in triplicate. Statistical analysis was done using ANOVA single factor ($P < 0.05$).

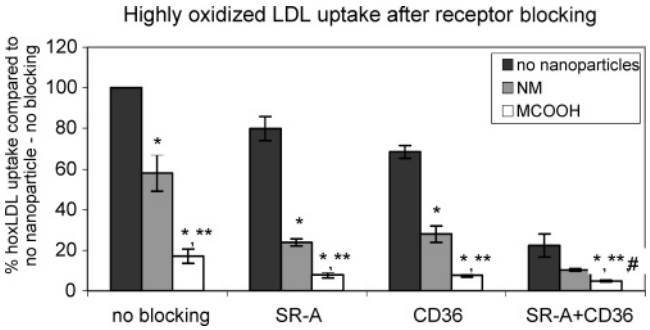

Figure 5. Scavenger receptor pathways involved in the nanoparticle-mediated inhibition of hoxLDL uptake. Cells were incubated with 10 μg/mL primary antibodies to SR-A and CD36 as well as a combination of the two for 30−45 min at 37 °C to block the respective receptors. Then, a mixture of fluorescently labeled hoxLDL-BODIPY and unlabeled nanoparticles was added to the cells for 2 h at 37 °C, in the presence of 10 μg/mL primary antibodies to avoid depletion during the incubation period. Controls of no nanoparticles and no receptor blocking were used. Lipoprotein uptake in each case was quantified using fluorescence microscopy and densitometry. The experiment was repeated 3−4 times. Statistical analysis was done using ANOVA single factor ($P < 0.05$). Single asterisk represents significant difference between that condition and no blocking/no nanoparticle condition, double asterisk between anionic and uncharged nanoparticle of the same receptor blocking condition and pound sign between some receptor blocking and no blocking within the same nanoparticle condition.

assemble into a micellar form. This macromolecule (i.e., PEG-COOH) was unable to inhibit hoxLDL uptake by macrophages, despite the presence of the anionic groups. The influence of the localized charge density was also confirmed by dose response studies performed to improve the efficiency of our nanoparticles in inhibiting oxidized LDL internalization by macrophages. At concentrations below the critical micelle concentration (10^{-7} M), where the macromolecules are unable to form micellar nanoparticles with increased charge density, highly oxidized LDL uptake was not inhibited, and the internalization levels were similar to the control lacking anionic nanoparticles.[23] Thus, the clustering of anionic charges in nanoscale micellar carriers improves their efficiency in inhibiting oxidized LDL uptake by macrophages.

One of the major findings of our study is that the chemical and structural features of the nanoparticles may allow interactions with multiple key scavenger receptors that mediate highly oxidized LDL uptake. The two predominant receptors involved in highly oxidized LDL uptake in macrophages are SR-A and CD36. Experiments with mice lacking both SR-A and CD36 receptors demonstrate that these two receptors account for the vast majority (75−90%) of modified LDL uptake and degradation.[12] A typical feature of the class A scavenger receptors is that they mediate the uptake and degradation of modified proteins and several polyanionic ligands,[5] even if they are not structurally related.[4,6] Binding to SR-A is mainly mediated through electrostatic interactions[31] between the lysine residues in its collagenous domain and negative charges on the ligands,[36] and this binding is likely the major interaction of the receptor with negatively charged highly oxidized LDL and with the anionic nanoparticles. On the other hand, interactions of ligands with CD36 are primarily lipid-based[31] and partly mediated via charge interactions, but it has also been shown that structure, hydrogen bonding, as well as lipophilic properties of the ligands also play a role.[19,37,38] A hydrophobic sequence (amino acids

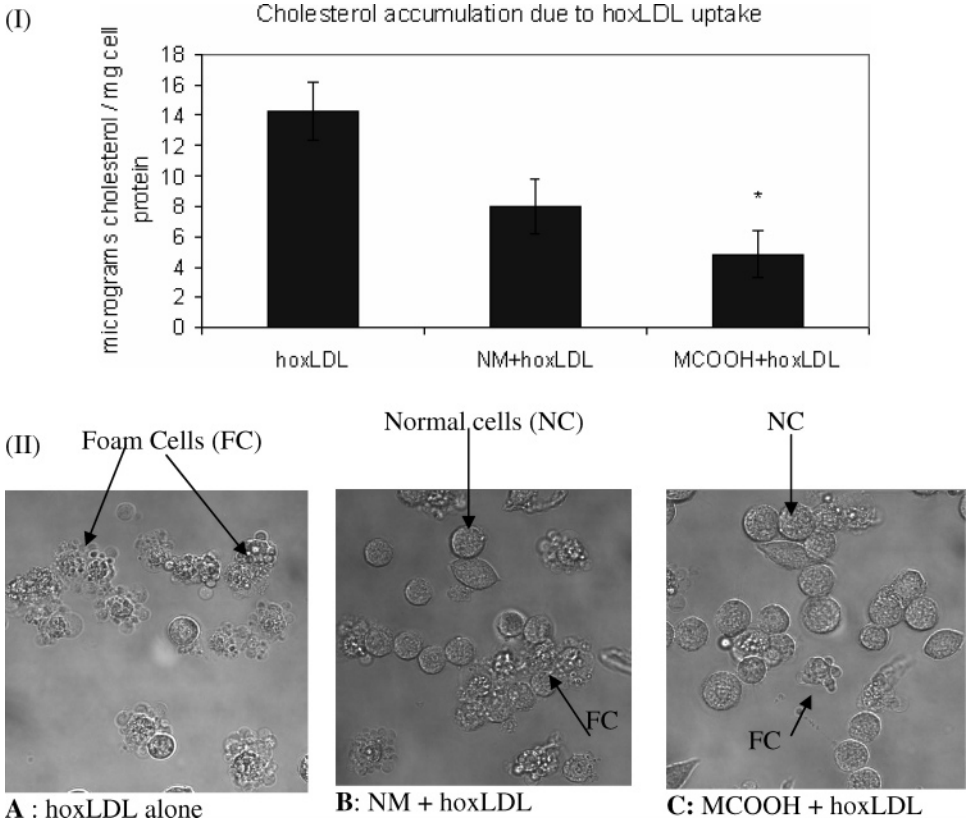

Figure 6. Cholesterol accumulation and foam cell formation. (I) Cells were incubated with 40 μg/mL hoxLDL for 12 h to allow for cholesterol accumulation. The lipids were then extracted with a mixture of hexane:2-propanol (3:2), and the total cholesterol was quantified by measuring a fluorescent product that directly correlates to the amount of cellular cholesterol. The data are averaged over 2 experiments done in triplicate. Statistical analysis was done using ANOVA single factor ($P < 0.05$). (II) Foam cell formation was assessed by cell morphology after incubation of cells with 40 μg/mL hoxLDL for 24 h in the absence (A) or presence of (B) NM or (C) MCOOH.

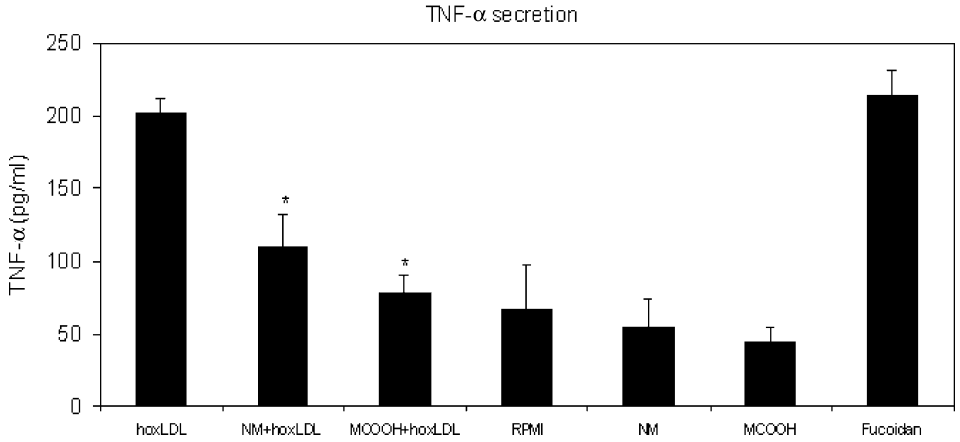

Figure 7. TNF-α secretion. Cells were incubated with 5 μg/mL hoxLDL for 6 h and the supernatants were collected for quantification of TNF-α secretion using ELISA. Fucoidan was used as a positive control. Data are representative of 3 independent experiments done in duplicate. Statistical analysis was done using ANOVA single factor ($P < 0.05$).

184−204) has been proposed to be membrane-associated or form hydrophobic pockets on the CD36 receptor.[39] These regions, in conjunction with the immunodominant domain (amino acids 155−183), may be mediating association of the nanoparticles with the receptor through a combination of charge-based and hydrophobic−hydrophobic interactions.

The anionic nanoparticles may interact with the scavenger receptors, blocking highly oxidized LDL binding and uptake. This hypothesis is supported by our experimental data indicating that SR-A is involved in both the uptake of anionic nanoparticles and of highly oxidized LDL. In contrast, CD36 has a minimal effect in basal nanoparticle internalization but is involved in nanoparticle−cell interactions and clearly mediates highly oxidized LDL uptake. Anionic nanoparticles may act as inhibitors of highly oxidized LDL uptake via scavenger receptor A and, potentially, CD36. Confirmation of anionic nanoparticle inhibition of uptake via scavenger receptors comes from our experiments where both anionic nanoparticles and highly oxidized LDL were present. The uncharged nanoparticles, which do not seem to interact with the scavenger receptors, elicited a basal level of reduction in hoxLDL internalization; the reduction is potentially due to inhibition of nonspecific internalization pathways, such as pinocytosis and lipid rafts.[40,41] The anionic nanoparticles cause a significant further decrease in hoxLDL

uptake that may be induced by competitive binding of the nanoparticles with the scavenger receptors mediating hoxLDL entry to the cells. Highly oxidized LDL uptake by macrophages was inhibited at a similar degree in the presence of anionic nanoparticles without receptor blocking as in simultaneous SR-A and CD36 blocking in the absence of nanoparticles. This inhibition is a strong indication that the anionic nanoparticle inhibitory effect occurs via SR-A and CD36 receptor blocking. Preconditioning of the cells with receptor specific antibodies to SR-A or CD36 did not elicit significant further inhibition, suggesting that the anionic nanoparticles similarly block hoxLDL entrance through these receptors. Simultaneous blocking of SR-A and CD36 with the respective antibodies in the presence of anionic nanoparticles further reduced hoxLDL uptake compared to other conditions within the anionic nanoparticle group as well as compared to the uncharged nanoparticles or to hoxLDL alone when both receptors were blocked. These results point to the potential higher affinity and specificity of the antibody−scavenger receptor binding compared to the anionic nanoparticles, as well as to the possibility of the carriers interacting with additional receptors mediating hoxLDL uptake such as macrosialin[11] and SR-PSOX (scavenger receptor for phosphatidylserine and oxidized lipoprotein).[42]

Apart from inhibiting uncontrolled hoxLDL uptake by macrophages, anionic nanoparticles also appear to control intracellular cholesterol accumulation thus reducing foam cell formation. Uncontrolled entrance of modified lipoproteins in macrophages leads to an increase in the total intracellular cholesterol that exists in the forms of free cholesterol and cholesteryl esters. Transported by LDL, cholesterol passes through the endosomes to the lysosomes, from which it either reaches the endoplasmic reticulum (ER) or the cell membrane. Excess cholesterol in the ER becomes esterified and is stored in the cytoplasm as lipid droplets.[43] Controlled oxidized LDL internalization by macrophages due to the presence of the anionic nanoparticles appears to have an effect on cholesterol accumulation that is reduced by 3-fold compared to the condition without nanoparticles. This internalization has a further effect in the foam cell phenotype of macrophages that is less pronounced in the presence of anionic nanoparticles.

Highly oxidized LDL, in addition to its ability to be taken up rapidly by macrophages to form foam cells, has many atherogenic properties including the upregulated secretion of inflammatory cytokines, such as tumor necrosis factor alpha (TNF-α) and interleukin-1β (IL-1β)[34,44−46] that influence atherogenesis. The macrophage-derived inflammatory cytokines cause endothelial cellular expression of procoagulant activity[34] and affect the migration,[47] proliferation, and apoptosis[48] of vascular smooth muscle cells. Various studies have shown that the uptake of low concentrations of oxidatively modified LDL activates macrophage secretion of inflammatory cytokines such as TNF-α.[17,34] In our studies, cell conditioning with hoxLDL increased the levels of basal TNF-α secretion by 3-fold, but in the presence of the nanoparticles, the oxLDL-induced secretion of TNF-α was lowered by more than 50%. Fucoidan, which induces cytokine secretion merely upon receptor binding and ligation,[34] contrasts with the anionic nanoparticles that did not induce upregulation of TNF-α secretion. Reports have shown that acetylated LDL and malondialdehyde-modified LDL, characteristic ligands of scavenger receptor A, did not induce TNF-α production upon binding to the receptor.[49] The reduced TNF-α secretion in the presence of the nanoparticles may be due to decreased oxidized LDL binding and uptake via receptor-mediated and low affinity nonspecific endocytosis, considering that the uncharged nanoparticles similarly had a significant effect. Decreased inflammatory TNF-α secretion by macrophages may inhibit migration of neighboring smooth muscle cells into the intima that can then overproliferate, thus, decreased TNF-α secretion may delay the progression of the plaque formation or intimal hyperplasia.

The overall implications of our study are that nanoscale biomaterials can be designed to control receptor-mediated uptake of the otherwise unregulated uptake of highly oxidized LDL. Consequently, the nanoparticles may limit the oxidized LDL-induced damage due to excessive cholesterol accumulation and secretion of atherogenic cytokines. Applications of these synthetic anionic nanoparticles include the management of vascular wall injury following balloon angioplasty and stenting to prevent restenotic episodes[50−52] where (i) inflammatory responses of intimal macrophages can further trigger vascular wall injury[2,48] and (ii) highly oxidized LDL uptake in smooth muscle cells leads to matrix remodeling and intimal hyperplasia.[53−55] An additional advantage of these multifunctional amphiphilic nanoparticles is their ability to water-solubilize hydrophobic antioxidants and/or drugs for localized delivery at sites of injury and inflammation.

Acknowledgment. This study was supported by a NSF-BES (0201788) grant, an American Heart Association Grant-in-Aid (9951060T; 0455823T) award to P.M., and a NSF-BES (9983272) grant to K.E.U. We thank Dr. Rene Rosenson-Schloss (Biomedical Engineering Department, Rutgers University) for valuable discussions on LDL internalization pathways and Dr. Lu Tian (Department of Chemistry and Chemical Biology, Rutgers University) for the synthesis of the nanoparticles.

References and Notes

(1) Li, A. C. *Nat. Med.* **2002**, *8* (11), 1235−42.
(2) Takahashi, Y.; Kinoshita, T.; Sakashita, T.; Inoue, H.; Tanabe, T.; Takahashi, K. *Adv. Exp. Med. Biol.* **2002**, *507*, 403−7.
(3) Lougheed, M.; Steinbrecher, U. P. *J. Biol. Chem.* **1996**, *271* (20), 11798−805.
(4) Zhang, H.; Yang, Y.; Steinbrecher, U. P. *J. Biol. Chem.* **1993**, *268* (8), 5535−42.
(5) Yla-Herttuala, S.; Hiltunen, T. P. *Atherosclerosis* **1998**, 137 Suppl, S81−8.
(6) de Winther, M. P. v. D. K.; Havekes, L. M.; Hofker, M. H. *Arterioscler. Thromb. Vasc. Biol.* **2000**, *20* (2), 290−7.
(7) Hiltunen, T. P.; Yla-Herttuala, S. *Atherosclerosis* **1998**, 137 Suppl, S81−8.
(8) Lougheed, M.; Lum, C. M.; Ling, W.; Suzuki, H.; Kodama, T.; Steinbrecher, U. *J. Biol. Chem.* **1997**, *272* (20), 12938−44.
(9) Nicholson, A. C.; Han, J.; Febbraio, M.; Silversterin, R. L.; Hajjar, D. P. *Ann. N.Y. Acad. Sci.* **2001**, *947*, 224−8.
(10) Febbraio, M.; Sheibani, N.; Schmitt, D.; Silverstein, R. L.; Hajjar, D. P.; Cohen, P. A.; Frazier, W. A.; Hoff, H. F.; Hazen, S. L. *J. Clin. Invest.* **2000**, *105* (8), 1095−108.
(11) Ramprasad, M. P., T. V.; Kondratenko, N.; Quehenberger, O.; Steinberg, D. *Proc. Natl. Acad. Sci. U.S.A.* **1996**, *93* (25), 14833−8.
(12) Kunjathoor, V. V.; Febbraio, M.; Podrez, E. A.; Moore, K. J.; Andersson, L.; Koehn, S.; Rhee, J. S.; Silverstein, R.; Hoff, H. F.; Freeman, M. W. *J. Biol. Chem.* **2002**, *277* (51), 49982−8.
(13) Berliner, J. A.; Heinecke, J. W. *Free Radical Biol. Med.* **1996**, *20* (5), 707−27.
(14) Brown, M. S.; Goldstein, J. L. *Annu. Rev. Biochem.* **1983**, *52*, 223−261.
(15) Steinberg, D. *J. Biol. Chem.* **1997**, *272* (22), 20963−20966.
(16) Sugano, R.; Yamamura, T.; Harada-Shiba, M.; Miyake, Y.; Yamamoto, A. *Atherosclerosis* **2001**, *158* (2), 351−7.
(17) Jovinge, S.; Ares, M. P.; Kallin, B.; Nilsson, J. *Arterioscler., Thromb. Vasc. Biol.* **1996**, *16* (12), 1573−9.
(18) Boullier, A.; Friedman, P.; Harkewicz, R.; Hartvigsen, K.; Green, S. R.; Almazan, F.; Dennis, E. A.; Steinberg, D.; Witztum, J. L.; Quehenberger, O. *J. Lipid Res.* **2005**, *46*, 969−976.
(19) Yoshiizumi, K.; Nakajima, F.; Dobashi, R.; Nishimura, N.; Ikeda, S. *Bioorg. Med. Chem.* **2002**, *10* (8), 2445−60.

(20) Lu Tian, L. Y.; Zhou, N.; Tat, H.; Uhrich, K. E. *Macromolecules* **2004**, *37* (2), 538−543.
(21) Djordjevic, J.; Barch, M.; Uhrich, K. E. *Pharm. Res.* **2005**, *22* (1), 24−32.
(22) Djordjevic, J.; Michniak, B.; Uhrich, K. E. *AAPS Pharm. Sci.* **2003**, *5* (4), E26.
(23) Chnari, E.; Nikitczuk, J. S.; Uhrich, K. E.; Moghe, P. V. *Biomacromolecules* **2006**, *7*, 597−603.
(24) Chnari, E.; Lari, H. B.; Tian, L.; Uhrich, K. E.; Moghe, P. V. *Biomaterials* **2005**, *26* (17), 3749−58.
(25) Oorni, K.; Pentikainen, M. O.; Annila, A.; Kovanen, P. T. *J. Biol. Chem.* **1997**, *272* (34), 21303−11.
(26) Chang, M. Y.; Potter-Perigo, S.; Wight, T. N.; Chait, A. *J. Lipid Res.* **2001**, *42*, 824−833.
(27) Patel, R. P.; Boersma, B. J.; Crawford, J. H.; Hogg, N.; Kirk, M.; Kalyanaraman, B.; Parks, D. A.; Barnes, S.; Darley-Usmar, V. *Free Radical Biol. Med.* **2001**, *31* (12), 1570−81.
(28) Esterbauer, H.; Striegl, G.; Puhl, H.; Rotheneder, M. *Free Radical Res. Commun.* **1989**, *6* (1), 67−75.
(29) Jiang, Z. Y.; Hunt, J. V.; Wolff, S. P. *Anal. Biochem.* **1992**, *31* (2), 384−9.
(30) el-Saadani, M.; Esterbauer, H.; el-Sayed, M.; Goher, M.; Nassar, A. Y.; Jurgens, G. *J. Lipid Res.* **1989**, *30* (4), 627−30.
(31) Wang, X.; Greilberger, J.; Ratschek, M.; Jurgens, G. *J. Pathol.* **2001**, *195* (2), 244−50.
(32) Jurgens, G.; Hoff, H. F.; Chisolm, G. M. 3rd; Esterbauer, H. *Chem. Phys. Lipids* **1987**, *45* (2−4), 315−36.
(33) Tian, L. *Novel Amphiphilic Macromolecules for Drug Delivery Applications: Design, Synthesis and Characterization.* Rutgers, The State University of New Jersey: New Brunswick, NJ, 2004.
(34) Hsu, H. Y.; Chiu, S. L.; Wen, M. H.; Chen, K. Y.; Hua, K. F. *J. Biol. Chem.* **2001**, *276* (31), 28719−30.
(35) Boullier, A.; Gillotte, K. L.; Horkko, S.; Green, S. R.; Friedman, P.; Dennis, E. A.; Witztum, J. L.; Steinberg, D.; Quehenberger, O. *J. Biol. Chem.* **2000**, *275* (13), 9163−9.
(36) Platt, N.; Gordon, S. *J. Clin. Invest.* **2001**, *108* (5), 649−54.
(37) Boullier, A.; Bird, D. A.; Chang, M. K.; Dennis, E. A.; Friedman, P.; Gillotre-Taylor, K.; Horkko, S.; Palinski, W.; Quehenberger, O.; Shaw, P.; Steinberg, D.; Terpstra, V.; Witztum, J. L. *Ann. N.Y. Acad. Sci.* **2001**, *947*, 214−22; discussion 222−3.
(38) Podrez, E. A.; Hoppe, G.; O'Neil, J.; Sayre, L. M.; Sheibani, N.; Hoff, H. F. *J. Lipid Res.* **2000**, *41* (9), 1455−63.
(39) Yamada, H.; Kazumi, Y.; Doi, N.; Otomo, K.; Aoki, T.; Mizuno, S.; Udagawa, T.; Tagawa, Y.; Iwakura, Y.; Yamada, Y. *J. Med. Microbiol.* **1998**, *47* (10), 871−7.
(40) Makoveichuk, E.; Castel, S.; Vilaro, S.; Olivecrona, G. *Biochim. Biophys. Acta* **2004**, *1686* (1−2), 37−49.
(41) Boren, J.; Lookene, A.; Makoveichuk, E.; Xiang, S.; Gustafsson, M.; Liu, H.; Talmud, P.; Olivecrona, G. *J. Biol. Chem.* **2001**, *276* (29), 26916−22.
(42) Kume, N.; Shimaoka, T.; Kataoka, H.; Hayashida, K.; Yonehara, S.; Kita, T.; Minami, M. *Ann. N.Y. Acad. Sci.* **2001**, *947*, 373−6.
(43) Maxfield, F. R.; Wustner, D. *J. Clin. Invest.* **2002**, *110* (7), 891−8.
(44) Mytar, B.; Gawlicka, M.; Szatanek, R.; Woloszyn, M.; Ruggiero, I.; Piekarska, B.; Zembala, M. *Inflammation Res.* **2004**, *53* (3), 100−6.
(45) Frostegard, J.; Huang, Y. H.; Ronnelid, J.; Schafer-Elinder, L. *Arterioscler., Thromb. Vasc. Biol.* **1997**, *17* (5), 963−8.
(46) Hultgardh-Nilsson, A.; Regnstrom, J.; Nilsson, J.; Jovinge, S. *Arterioscler., Thromb. Vasc. Biol.* **1997**, *17* (3), 490−7.
(47) Crisby, M.; Thyberg, J.; Nilsson, J.; Jovinge, S. *Arterioscler., Thromb. Vasc. Biol.* **1997**, *17* (10), 2225−31.
(48) Weissberg, P. L.; Bennett, M. R.; Boyle, J. J. *Arterioscler., Thromb. Vasc. Biol.* **2002**, *22* (10), 1624−30.
(49) Jozefowski, S.; Kobzik, L. *J. Leukocyte Biol.* **2004**, *76* (5), 1066−74.
(50) Sindermann, J. R.; Verin, V.; Hopewell, J. W.; Rodemann, H. P.; Hendry, J. H. *Cardiovasc. Res.* **2004**, *63* (1), 22−30.
(51) Tsuji, T.; Tamai, H.; Igaki, K.; Kyo, E.; Kosuga, K.; Hata, T.; Nakamura, T.; Fujita, S.; Takeda, S.; Motohara, S.; Uehata, H. *Int. J. Cardiovasc. Interventions* **2003**, *5* (1), 13−6.
(52) Gershlick, A. H. *Vasc. Med.* **1998**, *3* (3), 177−88.
(53) Wada, Y.; Sugiyama, A.; Yamamoto, T.; Naito, M.; Noguchi, N.; Yokoyama, S.; Tsujita, M.; Kawabe, Y.; Kobayashi, M.; Izumi, A.; Kohro, T.; Tanaka, T.; Taniguchi, H.; Koyama, H.; Hirano, K.; Yamashita, S.; Matsuzawa, Y.; Niki, E.; Hamakubo, T.; Kodama, T. *Arterioscler., Thromb. Vasc. Biol.* **2002**, *22* (10), 1712−9.
(54) Absood, A.; Furutani, A.; Kawamura, T.; Graham, L. M. *Am. J. Physiol.−Heart Circ. Physiol.* **2002**, *283* (2), H725−32.
(55) Absood, A.; Furutani, A.; Kawamura, T.; Graham, L. M. *Am. J. Physiol.−Heart Circ. Physiol.* **2004**, *287* (3), H1200−6.

BM0600872